

Cite this article as: Zhang Lei, Huang Yanfei, He Dongyu, et al. Effect of Steady Magnetic Field on Microstructure and Properties of NiCrBSi Coating by Supersonic Plasma Spraying[J]. Rare Metal Materials and Engineering, 2023, 52(01): 103-110.

ARTICLE

Effect of Steady Magnetic Field on Microstructure and Properties of NiCrBSi Coating by Supersonic Plasma Spraying

Zhang Lei^{1,2}, Huang Yanfei², He Dongyu², Guo Weiling², Li Guolu¹, Dong Tianshun¹

¹School of Materials Science and Engineering, Hebei University of Technology, Tianjin 300401, China; ²National Key Laboratory for Remanufacturing, Army Academy of Armored Forces, Beijing 100072, China

Abstract: The NiCrBSi coating was sprayed onto the 45 steel under a steady magnetic field. The microstructure, mechanical properties, and friction and wear properties of coatings were studied. In the steady magnetic field, the coating porosity decreases dramatically. No new phase forms, but the preferred orientation occurs for the γ -Ni, FeNi₃, and Ni₃Si₂ phases. Moreover, the magnetic domains within the coating become more active and more ordered with subtle variations in external magnetic fields. The microhardness of the cross section of coating increases significantly, the residual stress on the surface fluctuates obviously, and the wear amount of the coating decreases by nearly 13.6%. Results show that a steady magnetic field can improve the coating quality effectively. Besides, the mechanism of property enhancement of Ni-based coating by spraying under steady magnetic field was discussed.

Key words: steady magnetic field; supersonic plasma spraying; Ni-based coating; electromagnetic stirring; wear resistance

Magnetic field-assisted machining is an advanced non-contact external energy field-assisted machining method on the basis of Maxwell electromagnetic field theory^[1-2]. In recent years, the magnetic field-assisted coating or thin film deposition has been widely researched. Through the magnetic field-assisted laser cladding, Zhou et al^[3] melted the magnesium alloy surface and found that the laser cladding can generate a highly uniform layer with fine grains, resulting in the significantly improved microhardness, wear resistance, and corrosion resistance of the coating. Zhang et al^[4] reported that adding a longitudinal alternating magnetic field with variable frequency in the laser cladding process can increase the uniformity of the element distribution, thereby increasing the plastic toughness of the coating. Jiang et al^[5] prepared the jet-electrodeposited nickel-silicon carbide composite coating by the magnetic field-assisted method. It is revealed that the magnetic field-assisted method can reduce the cellular protrusion and improve the the coating smoothness. In addition, the magnetic field-assisted method can strengthen

the wear resistance and improve the corrosion resistance of nickel-silicon carbide coatings. Magnetic force F_m has an important effect on the mass transfer in magnetic electrodeposition process: it can improve the deposition rates and obtain smaller grain sizes^[6]. Zhou et al^[7] studied the influence of strong parallel magnetic field on the electrodeposition of silicon nanoparticles into the iron matrix and found that the silicon particles can be easily deposited with a high concentration under low current density and parallel magnetic field of 2 T.

It is also reported that when the steady magnetic field is added in the detonation spraying process, the coating porosity significantly reduces to less than 3%, and the adhesion capacity increases to 7 MPa, which is five times higher than that of the coating prepared without magnetic field^[8]. Tharajak et al^[9] found that the application of steady magnetic field parallel to the spraying direction can improve the crystallinity and microhardness of poly(ether-ether-ketone) coatings. This is because the steady magnetic field induces orientation and

Received date: March 15, 2022

Foundation item: National Natural Science Foundation of China (52130509); Key Basic Research Project of Foundation Strengthening Plan (2019-JCJQ-ZD-302)

Corresponding author: Li Guolu, Ph. D., Professor, School of Materials Science and Engineering, Hebei University of Technology, Tianjin 300401, P. R. China, E-mail: liguolu@hebut.edu.cn

Copyright © 2023, Northwest Institute for Nonferrous Metal Research. Published by Science Press. All rights reserved.

alignment of the polyether-ether-ketone molecules. However, the magnetic field-assisted thermal spraying has been rarely researched, and the mechanism of coating strengthening is not clear. Therefore, the magnetic field-assisted spraying was investigated in this research.

Plasma spraying technique is a widely used method for surface strengthening due to its convenient operation, low cost, high efficiency, and achievement of high quality of coatings^[10-21]. The coatings prepared in a steady magnetic field environment are named as SMF coatings, and those prepared in a non-magnetic field environment are named as NMF coatings. During the steady magnetic field-assisted supersonic plasma spraying, the magnetic field can affect the solidification process of coating, thereby improving the coating properties. The steady magnetic field-assisted supersonic plasma spraying technique belongs to the processing technology of auxiliary materials. However, it is rarely researched and lacks quantitative analysis. Therefore, it is of great significance to study the preparation of coatings by steady magnetic field-assisted supersonic plasma spraying technique.

In this research, the NiCrBSi coating was sprayed onto the 45 steel under a steady magnetic field. The microstructure, mechanical properties, and friction and wear properties of the SMF coatings and the NMF coatings were compared. In addition, the mechanism of property enhancement of the Ni-based coating by spraying under steady magnetic field was discussed.

1 Experiment

The powder used in this research was commercial NiCrBSi (Ni60A) powder. The content of each element in powder was analyzed by inductive-coupled plasma (ICP) emission spectrometer, as shown in Table 1. The microstructure of NiCrBSi powder was observed by ZEISS GeminiSEM300 scanning electron microscope (SEM), as shown in Fig. 1. The powder has good sphericity and the average particle size is about 20–40 μm . The 45 steel was used as the substrate with size of 35 mm \times 25 mm \times 9 mm. SiC sandblasting was conducted before spraying to increase the contact area between the coating and the substrate.

The coating specimens were prepared by XFQ-HVSP-800 supersonic plasma spraying equipment. Hydrogen was used as the main gas to provide enthalpy, and the argon was used as the protective gas to prevent excess oxidation of powder droplets. Meanwhile, the high-speed argon plasma produced by argon ionization could effectively reduce the coating porosity and improve the bonding strength. The main supersonic plasma spraying parameters are shown in Table 2. The equipment was coupled with a cold water circulation system to cool the spray gun, which was driven by the

Table 1 Main element composition of NiCrBSi powder (wt%)

Cr	Fe	B	Si	Ni
16.29	5.34	3.53	2.17	Bal.

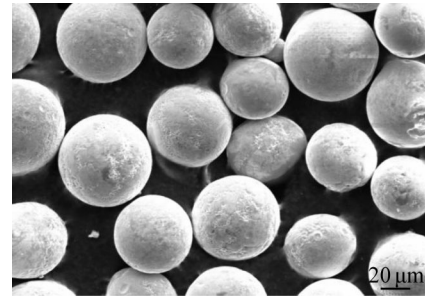


Fig.1 SEM microstructure of NiCrBSi powder

YASKAWA mechanical arm. The steady magnetic field in this research was provided by a commercial neodymium magnet. The size of a single magnet was 77 mm \times 57 mm \times 31.5 mm. In this research, the multiple neodymium magnets were superimposed to form a synthetic magnetic field to ensure the magnetic field strength.

Fig. 2 shows the schematic diagram of the supersonic plasma spraying experiment. The magnets were separated in cages made of 304 stainless steel and the 45 steel plate with the thickness of 3 mm was placed above them to conduct the magnetic force. The specimen was placed on the 45 steel plate for spraying. Before spraying, the Gauss meter was used to measure the magnetic induction intensity of the specimen position. The cooling water tanks were placed outside the cage.

The specimen microstructure was observed by SEM. ImagePro software was used to determine the coating porosity. The phase composition of NiCrBSi powder and coating prepared in a steady magnetic field with different field strengths was analyzed by BRUCKER D8 ADVANCE X-ray diffractometer (XRD, Cu target, $\lambda=0.154\ 06\ \text{nm}$, tube current of 40 mA, tube voltage of 40 kV, scanning angle of 30°–80°, scanning rate of 2°/min).

Finnish X-Stress Robot X-ray stress analyzer (Cr target, tube current of 6.7 mA, tube voltage of 30 kV, test angle of

Table 2 Main process parameters of supersonic plasma spraying

Voltage/ V	Current/ A	H ₂ flow/ L·min ⁻¹	Ar flow/ L·min ⁻¹	Powder feeding rate/g·min ⁻¹
125	430	13.0	120	2.73

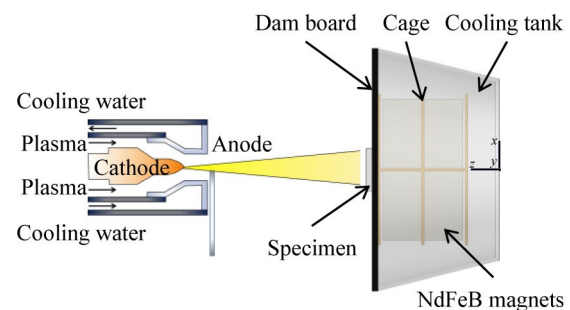


Fig.2 Schematic diagram of supersonic plasma spraying experiment

-45° – 45° , spot size of 3 mm, exposure for 5 s) was used to measure the residual stress on the coating surface. Vickers microhardness was measured by ShimadzuMV-2T Vickers microhardness tester with a load of 1.96 N and holding time of 10 s. The hysteresis loops of the coatings prepared with and without steady magnetic fields were analyzed by MMPS-3 Quantum Design.

The wear resistance of the coatings was evaluated by the UMT (ball-on-plate) friction and wear tester. GCr15 hardened steel balls were used as friction pair with microhardness of 62 HRC, diameter of 4 mm, and surface roughness R_a of 0.8 μm . Before the tests, the specimen was cut into the one with size of 35 mm \times 25 mm \times 9 mm by wire electrode cutting device and then ground and polished to $R_a=1.6 \mu\text{m}$. For the wear tests, the load was 30 N, the duration was 30 min, the frequency was 10 Hz, and the amplitude was 5 mm. The wear zone was located in the specimen center. To reduce the influence of circular arc on the wear test results, the grinding ball moved along a specific axis of specimen. After the wear tests, the wear properties of coatings were characterized by Brooke white light interferometer contour (GT series).

2 Results and Discussion

2.1 Cross-section morphology of coatings

The cross-section morphologies of the NiCrBSi coatings prepared with and without steady magnetic field are shown in Fig.3. According to Fig.3a, pores and unmelted particles exist in the sprayed NMF coating. As shown in Fig.3b, although there are unmelted particles inside the SMF coating, the number and the diameter of pores significantly reduce. The statistical results show that the coating porosity decreases from 6.9% to 0.9% after application of steady magnetic field. In addition, the surface of SMF coating is obviously smoother

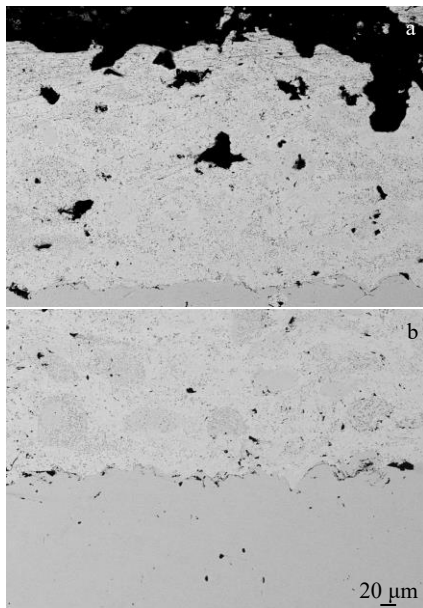


Fig.3 Cross-section morphologies of NMF (a) and SMF (b) NiCrBSi coatings

than that of NMF coating.

2.2 Phase composition of coatings

Fig. 4 shows XRD patterns of SMF and NMF NiCrBSi coatings. As shown in Fig. 4, the characteristic peaks of the two coatings are basically the same. Both the coatings are composed of γ -Ni, Ni₃Fe, CrB, Cr₃B₃, and Ni₃Si₂ phases, indicating that the introduction of steady magnetic field does not change the phase composition of NiCrBSi coating. However, the peak intensity of each phase increases in SMF coating, especially at $2\theta=44.3^{\circ}$, compared with that of NMF coating. It is inferred that the grains are preferentially oriented on specific crystal planes in SMF coating. When the diffraction angle is 40° – 50° , the diffusion of diffraction peaks can be observed in NMF coating, while it is not obvious in SMF coating. This is because the plasma spraying is characterized by rapid cooling, which causes melted or semi-melted particles to solidify before crystallization, leading to the formation of amorphous components.

2.3 Microhardness

Fig. 5 shows the microhardness of the cross-section of NiCrBSi coatings prepared with and without steady magnetic field. The microhardness of both two coatings is significantly higher than that of the 45 steel substrate.

The microhardness of NMF NiCrBSi coating is 5880–7840 MPa and the average microhardness of the coating is 7330.3 MPa. The microhardness of SMF NiCrBSi coating increases significantly and its average microhardness is 8683.8 MPa,

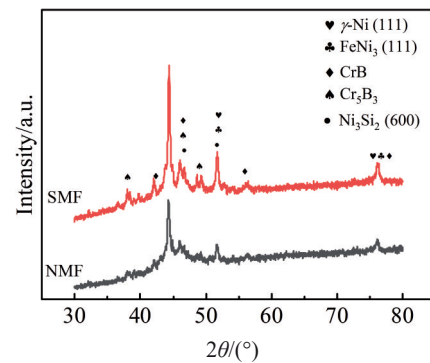


Fig.4 XRD patterns of NMF and SMF NiCrBSi coatings

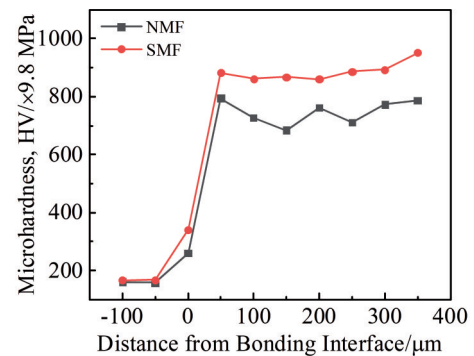


Fig.5 Microhardness of NMF and SMF NiCrBSi coatings

which is nearly 18.5% higher than that of NMF coating. This result indicates that the application of a steady magnetic field affects the microhardness of NiCrBSi coating.

2.4 Residual stress on coating surface

Fig.6 shows the residual stress range along *X* direction and *Y* direction on NMF and SMF NiCrBSi coating surfaces. As shown in Fig.6a, along *X* direction, the average residual stress on the surface of NMF coating is -42.9 MPa, while that on the surface of SMF coating is -58.1 MPa, indicating the compressive stress. Two outliers can be observed above and below the residual stress range of the NMF coating, which indicates that the residual stress gradient on the coating surface is too large to be included in the chamber and it is treated as an outlier. The length of the chamber does not accurately reflect the stress gradient range, so the variance of the residual stress of different specimens is calculated. The variance decreases from

2366.5 to 1162.8, which suggests that the residual stress on the SMF coating surface is more stable. This phenomenon is beneficial to improve the bonding strength of NiCrBSi coating. According to Fig. 6b, the average residual stress of NMF coating is -40.4 MPa with variance of 3395.2. The average residual stress on the surface of SMF coating is significantly reduced to -0.6 MPa, and the variance is 618.15, indicating that the application of steady magnetic field promotes the release of residual stress on the coating surface along *Y* direction. It can be observed that an outlier also appears above the residual stress range of the SMF coating. But according to the variance value, it can be considered that the residual stress gradient of the specimen is very small.

The variation of residual stress at different positions on the coating surface is shown in Fig.7. In Fig.7a, the residual stress of the NMF coating surface along *X* direction changes from

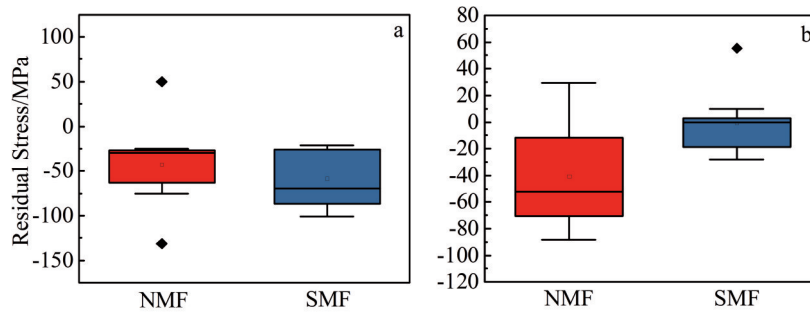


Fig.6 Residual stress distribution along *X* direction (a) and *Y* direction (b) of NMF and SMF NiCrBSi coatings

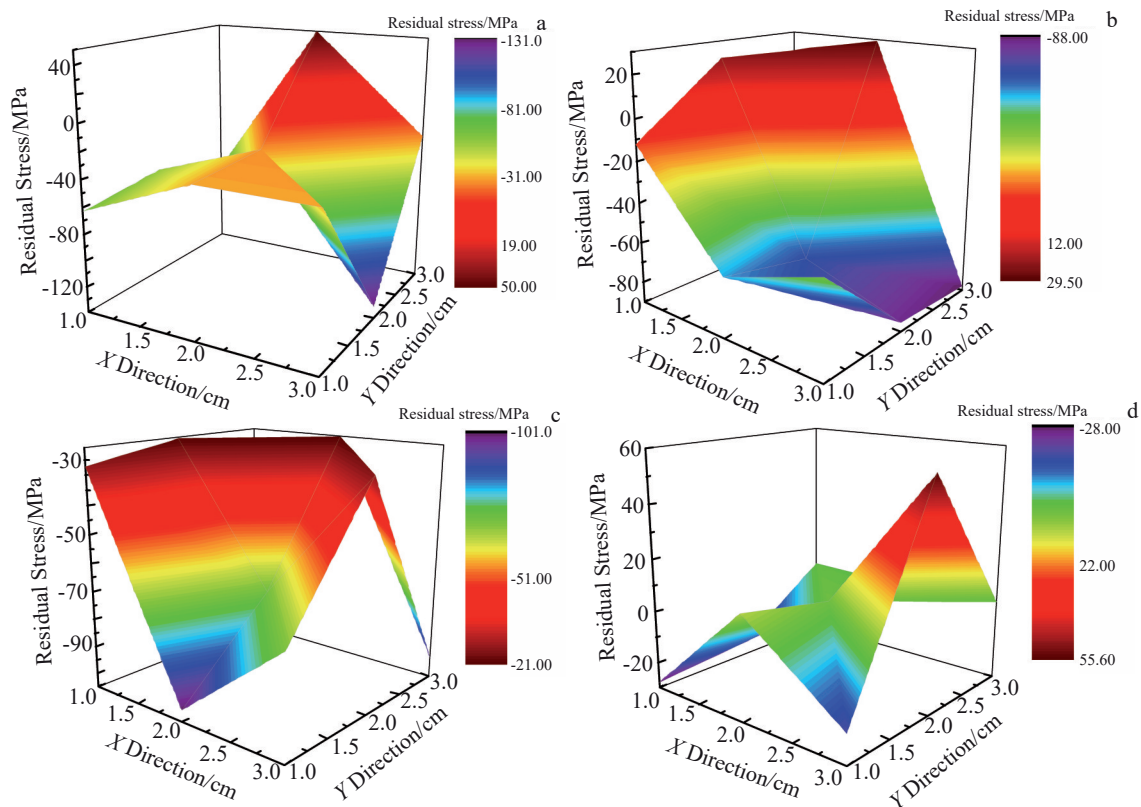


Fig.7 Residual stress along *X* direction (a, c) and *Y* direction (b, d) on surface of NMF (a, b) and SMF (c, d) NiCrBSi coatings

-131 MPa to 50 MPa. After the application of a steady magnetic field, the residual stress along X direction changes from -101 MPa to -20 MPa, as shown in Fig.7c. According to Fig.7b and 7d, the residual stress on the NMF coating surface along Y direction fluctuates from -88.0 MPa to 29.5 MPa, while it ranges from -28.0 MPa to 55.5 MPa in SMF coating. In addition, the residual stress always presents a steep-slope distribution, which is related to the solidification sequence of the coating.

2.5 Vibrating sample magnetometer analysis

Magnetic induction intensity M -magnetic strength H curves of SMF and NMF NiCrBSi coatings are shown in Fig.8. The internal-induced magnetic field of the two coatings varies with the external magnetic field. When H is less than 79.6 MA/m, the curve slope of SMF coating is always larger than that of NMF coating, indicating that the coating prepared under the steady magnetic field environment is more sensitive to the variation of external magnetic field. When H is more than 79.6 MA/m, the magnetic induction intensity of the two coatings is relatively stable, and there is no significant change. The magnetic saturation value of SMF coating is close to $\pm 42 \text{ A}\cdot\text{m}^2/\text{g}$, while the maximum value of NMF coating is only $\pm 18 \text{ A}\cdot\text{m}^2/\text{g}$.

The coercivity locates at the intersection point of the curve and X -axis, and the remanence locates at the intersection point of the curve and Y -axis^[22]. The coercivity in residual magnetization of the two coatings can be obtained from Fig.8b and Table 3. After application of steady magnetic field, the coercivity of coating decreases from 3203.90 kA/m to 1158.18 kA/m. The remanent magnetization of SMF coating

Table 3 Characteristic points in H - M curves of NMF and SMF NiCrBSi coatings

Specimen	Characteristic point	Coordinate in Fig.8b
NMF coating	M_N	(0, 2.47)
	H_N	(3203.90, 0)
SMF coating	M_S	(0, 3.24)
	H_S	(1158.18, 0)

increases to $3.24 \text{ Am}^2/\text{g}$, compared with that of NMF coating ($2.47 \text{ Am}^2/\text{g}$). This result indicates that the magnetic domains in the SMF coating are more regular and ordered and the residual magnetization is stronger after the application of steady magnetic field. Meanwhile, the magnetic domains inside the coating become more active and more sensitive to the subtle changes in the external magnetic field.

2.6 Wear resistance of coatings

Fig. 9 shows the friction coefficient of NMF and SMF NiCrBSi coatings. It can be seen that the friction coefficient of SMF coating is always lower than that of the NMF coating. The friction coefficient of NMF coating is stable between 0.45 -0.47 throughout the whole process. Within 400 s, the friction coefficient of SMF coating is stable at about 0.4. After 400 s, the friction coefficient of SMF coating increases gradually, but it is still lower than that of NMF coating.

The morphology analysis results further confirm the difference in wear volume between NMF and SMF NiCrBSi coatings, as shown in Fig. 10. It can be seen that the wear width of the SMF coating decreases by nearly $200 \mu\text{m}$, while the wear length does not change significantly. However, the wear depth of SMF coating is only $38 \mu\text{m}$, while NMF coating has the wear depth of $47 \mu\text{m}$. The three-dimensional morphometry results show that the wear volume of SMF coating is 0.114 mm^3 and that of NMF coating is 0.132 mm^3 , presenting a reduction of about 13.6%. Therefore, the application of steady magnetic field promotes the formation of stable wear phase, resulting in the decreased wear. This phenomenon may also be related to the increased coating microhardness.

2.7 Mechanism of coating strengthening

Each specimen was sprayed 10 times. Therefore, when the spraying was conducted on the specimen surface, the high-

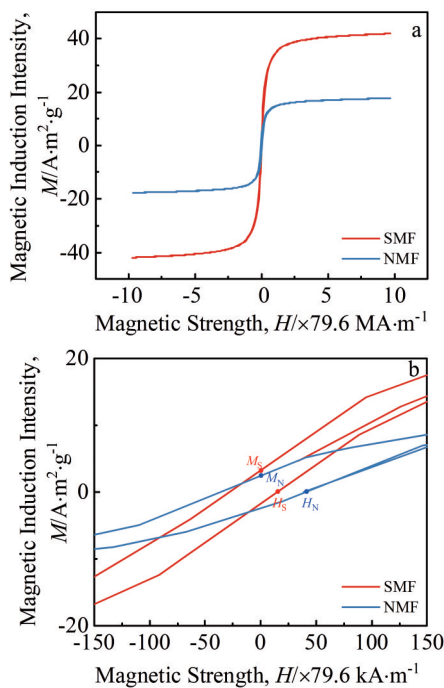


Fig.8 Magnetic induction intensity M -magnetic strength H curves of SMF and NMF NiCrBSi coatings with $H = [-10, 10] \times 79.6 \text{ MA/m}$ (a) and $H = [-150, 150] \times 79.6 \text{ kA/m}$ (b)

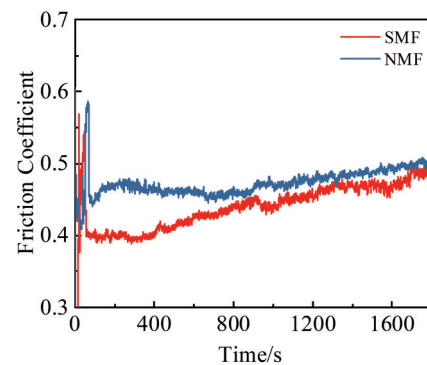


Fig.9 Friction coefficient of NMF and SMF NiCrBSi coatings

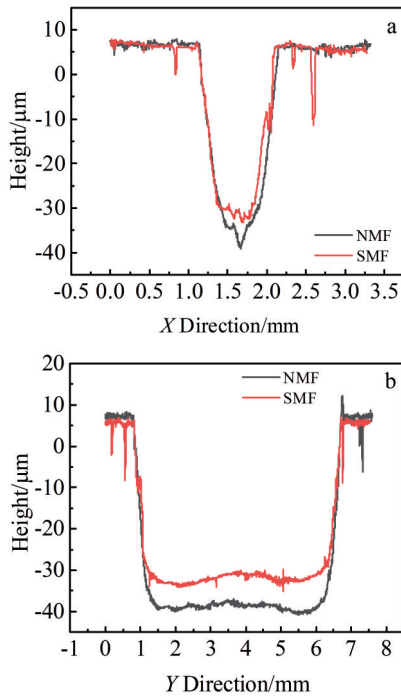


Fig.10 Wear morphologies along X direction (a) and Y direction (b) of NMF and SMF NiCrBSi coatings

temperature flame flow would melt the coating, i. e., a temporary molten pool was formed on the specimen surface within 2–3 s. Remelting treatment can effectively reduce the coating porosity^[23–26]. Without the magnetic field, the molten droplet rapidly cools down and forms a large number of dendrites after deposition on the substrate. The dendrites melt and crystallize again and again during repeated spraying until the temperature completely drops to room temperature. The anisotropy of dendrites causes the poor performance of NMF coatings.

However, when the coating is sprayed in a steady magnetic field, the coating forming process changes. Fig. 11 shows the melt model of the specimen surface when the coating is prepared in a steady magnetic field environment. Under the action of the steady magnetic field, the melt on the specimen surface firstly generates an inside induced current, and then moves directionally under the action of Lorentz force. On the one hand, the melt convection can release the gas inside the melt and reduce the coating porosity. The flowing melt, on the other hand, breaks the internal dendrites into pieces and transfers them into the melt. With decreasing the temperature, these fragments grow into a large number of fine grains.

Electron backscattered diffraction (EBSD) analysis also provides strong evidence for the grain refinement. As shown in Fig. 12a, the grain diameter distribution in NMF coating is relatively dispersed, and there are large grains with diameter more than 3.5 μm . The grains with diameter of less than 1 μm in NMF coating account for 53%, and those with diameter of less than 0.5 μm account for 46%. However, in SMF coating, the grain diameter is generally less than 1 μm . The grains with diameter of less than 1 μm account for 87%, and those with

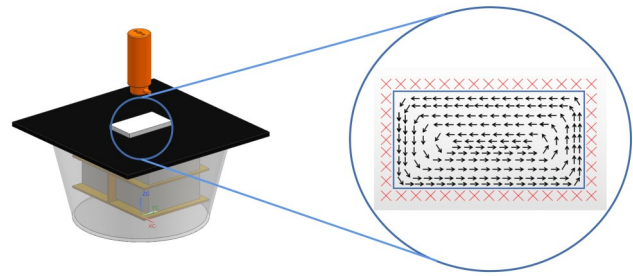


Fig.11 Schematic diagram of melt model of coating surface under steady magnetic field

diameter of less than 0.5 μm account for 66%. According to Holpage formula, the mechanical properties of the material will be enhanced when the grains are refined^[27–28]. The improved microhardness of SMF coating can also be explained.

Fig. 12b shows the grain boundary angle distributions in NMF and SMF coatings. It can be seen that the proportion of the low angle grain boundaries inside the two coatings is very similar (4% in NMF coating and 5% in SMF coating). The difference is obvious when the grain boundary misorientation is 30°–50°, which is in accordance with the common sense in crystallography. However, the grain boundaries with misorientation angle of 42.05° account for 31% in SMF coating, while those account for only 18% in NMF coating, indicating an increase of nearly 13%. These changes affect the grain boundary migration in the coating and then influence the plastic deformation ability of coating, thereby resulting in the better friction and wear properties of SMF coatings. Different extents of atomic arrangement distortion and grain boundary energies exist in the interface of high angle grain boundaries. With increasing the phase difference, the atomic arrangement distortion and grain boundary energy are increased. When the grain boundary angle increases to 86.55°, its proportion is 8% in NMF coating and 5% in SMF coating. The large number of high angle grain boundaries leads to the poor performance of NMF coatings. However, when the misorientation angle of grain boundary is about 60°, the proportion of this grain boundary in NMF coating is low (10%) and that in SMF coating is high (16%). However, the performance of SMF coating is still better than that of NMF coating. This is because for face-centered cubic metals, such as Ni, 60° is an important lattice parameter, which indicates the slight atomic alignment distortion and low grain boundary energy.

The introduction of a magnetic field causes magnetically sensitive elements, such as Cr, to move along the induction direction towards the poles. Fig. 13 shows the analysis results of energy dispersive spectrometer (EDS). Without the magnetic field, the Cr phase distribution in the NMF coating is not uniform. After application of a steady magnetic field, the Cr phase moves under the action of the magnetic field, because Cr has stronger ferromagnetism, compared with Ni, B, and Si elements. Local uniform distribution of the Cr phase is formed inside the SMF coating, resulting in the overall

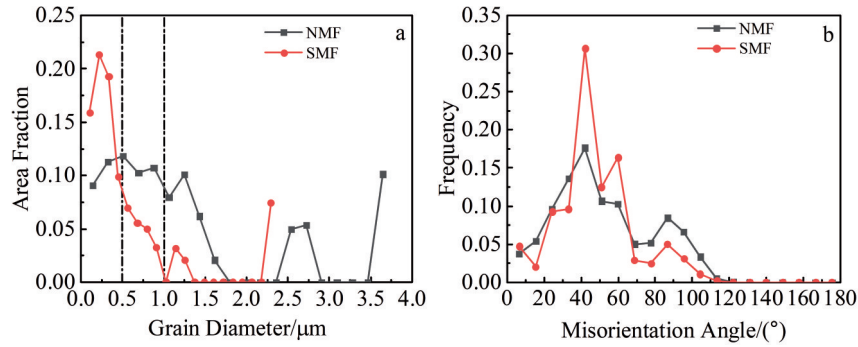


Fig.12 Grain diameter distribution (a) and grain boundary angle distribution (b) of NMF and SMF NiCrBSi coatings

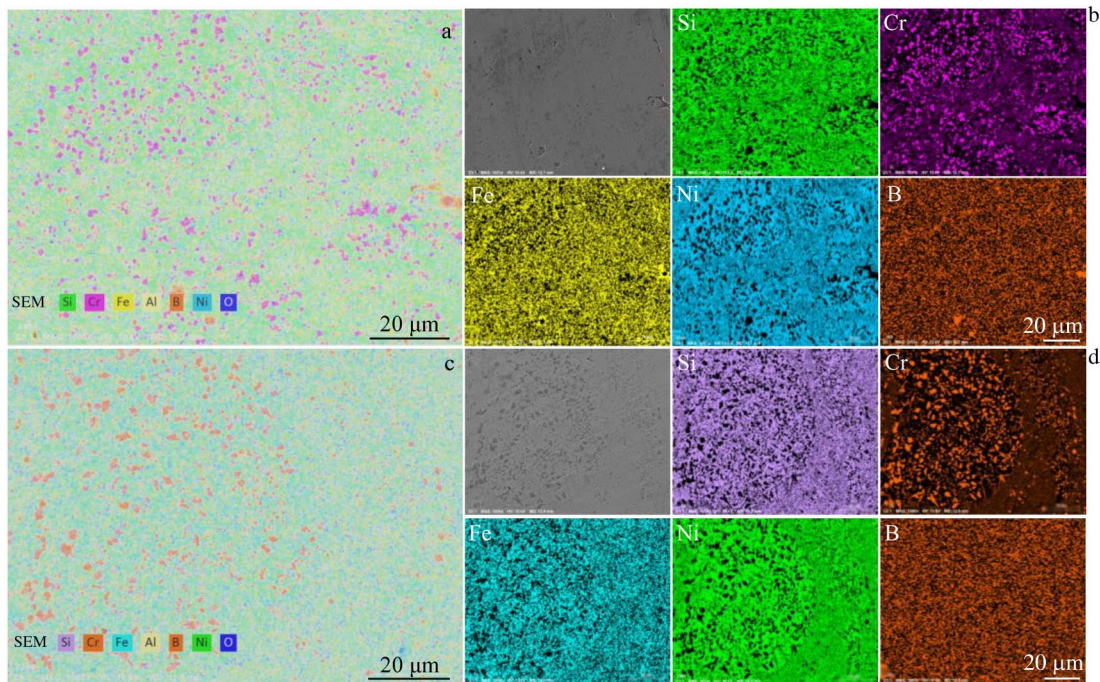


Fig.13 EDS element distributions of SMF (a, b) and NMF (c, d) of NiCrBSi coatings

strengthening effect. The uniform distribution of Cr phase also improves the wear resistance of the coatings. In addition, the uniform distribution of Cr phase also leads to the lower porosity of the coating prepared with a steady magnetic field.

The residual stress in the coating is mainly categorized as quenching stress, thermal stress, and stress concentration caused by the cavity^[29]. The quenching stress is caused by the rapid cooling of molten droplet when it is deposited on the substrate. The thermal stress is caused by the inhomogeneity of the coating during solidification. The droplet does not immediately solidify after reaching the matrix, but its solidification process is short. The introduction of the magnetic field can prolong the curing time and reduce the melt cooling gradient, thus reducing the residual stress of the coating. The decrease in coating porosity is also an important reason for the decrease in the residual stress of coating. The decreased porosity not only increases the inner density of the coating, but also

reduces the stress concentration of the coating.

3 Conclusions

1) For the NiCrBSi coating prepared in a steady magnetic field, the porosity and residual stress are decreased and the microhardness is increased. The magnetic domains inside the coating become more active and more ordered with slight changes in the external magnetic field. The wear resistance of NiCrBSi coating prepared in a steady magnetic field is better than that without steady magnetic field, and the wear volume of the coating decreases by nearly 13.6%.

2) The mechanism of coating strengthening in a steady magnetic field is that a molten pool forms on the coating surface during spraying, and the melt moves directionally under the action of the magnetic field, leading to the grain refinement. In addition, the Cr phase is homogenized under the action of the magnetic field.

References

- 1 Crane P F. *Annals of Science*[J], 1954, 10(4): 359
- 2 Markov M B, Parotkin S V. *Mathematical Models and Computer Simulations*[J], 2021, 13(2): 254
- 3 Zhou Jianzhong, Xu Jiale, Huang Shu et al. *Surface and Coatings Technology*[J], 2017, 309: 212
- 4 Zhang Qi, Zhang Peilei, Yan Hua et al. *Philosophical Magazine Letters*[J], 2020, 100(2): 86
- 5 Jiang Wei, Shen Lida, Qiu Mingbo et al. *Journal of Alloys and Compounds*[J], 2018, 762: 115
- 6 Yu Y D, Cao Y, Li M G et al. *Materials Research Innovations*[J], 2014, 18(4): 314
- 7 Zhou Pengwei, Zhong Yunbo, Wang Huai et al. *Applied Surface Science*[J], 2013, 282: 624
- 8 Dovgal A, Pryimak L, Trofimov I. *Eastern-European Journal of Enterprise Technologies*[J], 2016, 6(5): 33
- 9 Tharajak J, Palathai T, Sombatsompom N. *Wear*[J], 2017, 372–373: 68
- 10 Wang L, Fu Q G, Liu N K et al. *Surface Engineering*[J], 2016, 32(7): 508
- 11 Zhang J J, Wang Z H, Lin P H et al. *Surface Engineering*[J], 2012, 28(5): 345
- 12 Yang Y, Li K Z, Zhao Z G et al. *Advances in Applied Ceramics*[J], 2016, 115(8): 473
- 13 Wang Lu, Fu Qiangang, Zhao Fengling. *Surface and Coatings Technology*[J], 2017, 313: 63
- 14 Jiang Chaoping, Liu Wangqiang, Wang Gui et al. *Surface Engineering*[J], 2017, 34(8): 634
- 15 Singh H, Prakash S, Puri D et al. *Journal of Materials Engineering and Performance*[J], 2006, 15(6): 729
- 16 Zhang Yulei, Hu Heng, Zhang Pengfei et al. *Surface and Coatings Technology*[J], 2016, 300: 1
- 17 Kuleshov N, Dolgov N, Smirnov I et al. *Applied Mechanics and Materials*[J], 2020, 897: 61
- 18 He Pengfei, Ma Guozheng, Wang Haidou et al. *Journal of Materials Science and Technology*[J], 2021, 87: 216
- 19 Ma Guozheng, Chen Shuying, He Pengfei et al. *Surface and Coatings Technology*[J], 2019, 358: 394
- 20 Borisov A M, Vostrikov V G, Polyansky M N et al. *Journal of Surface Investigation: X-ray, Synchrotron and Neutron Techniques*[J], 2015, 9(2): 248
- 21 Caliaro F R, Miranda F S, Reis D A P et al. *Journal of Thermal Spray Technology*[J], 2017, 26(5): 880
- 22 Xu Jilin, Xiao Qifei, Mei Dingding et al. *Rare Metal Materials and Engineering*[J], 2018, 47(4): 1059
- 23 Liu Jingtao, Hou Jixin, Zhang Xiaorong et al. *Rare Metal Materials and Engineering*[J], 2017, 46(2): 296
- 24 Guan Zhousen, Wang Wenxian, Cui Zeqin et al. *Rare Metal Materials and Engineering*[J], 2015, 44(7): 1597
- 25 Liu Hailang, Wang Bo, Qi Zhengwei et al. *Rare Metal Materials and Engineering*[J], 2018, 47(11): 3338
- 26 Chang Fa, Zhou Kesong, Tong Xin et al. *Rare Metal Materials and Engineering*[J], 2017, 46(3): 577
- 27 Jin Qiaoling, Wang Haidou, Li Guolu et al. *Rare Metal Materials and Engineering*[J], 2017, 46(10): 2857
- 28 Kong Dejun, Wang Jinchun, Fu Guizhong et al. *Rare Metal Materials and Engineering*[J], 2015, 44(6): 1314
- 29 Kuroda S, Clyne T W. *Thin Solid Films*[J], 1991, 200(1): 49

稳恒磁场对超音速等离子喷涂 NiCrBSi 涂层组织和性能的影响

张磊^{1,2}, 黄艳斐², 何东昱², 郭伟玲², 李国禄¹, 董天顺¹

(1. 河北工业大学 材料科学与工程学院, 天津 300401)

(2. 陆军装甲兵学院 装备再制造技术国防科技重点实验室, 北京 100072)

摘要: 在稳恒磁场作用下, 在 45 钢上喷涂了 NiCrBSi 涂层, 并研究了 NiCrBSi 涂层的组织、力学性能和摩擦磨损性能。在稳恒磁场条件下, 涂层的孔隙率显著降低, 没有形成新物相, 但 γ -Ni、FeNi₃、Ni₃Si₂ 相中出现了择优取向。此外, 涂层内的磁畴变得更为活跃, 更容易随着外部磁场的细微变化而有序排列。涂层截面显微硬度显著提高, 表面残余应力波动明显, 涂层的磨损量降低了近 13.6%。实验结果表明, 稳恒磁场可以有效地改善涂层质量。此外, 探讨了稳定磁场下喷涂提高 Ni 基涂层性能的机理。

关键词: 稳恒磁场; 超音速等离子喷涂; Ni 基涂层; 电磁搅拌; 耐磨性能

作者简介: 张磊, 男, 1995 年生, 博士, 河北工业大学材料科学与工程学院, 天津 300401, E-mail: zhangl_ziyu@163.com